

# Boosting size-selective hydrogen combustion in presence of propene using controllable metal clusters encapsulated in zeolite

Yuling Shan, Zhijun Sui\*, Yian Zhu, Jinghong Zhou, Xinggui Zhou and De Chen\*

**Abstract:** A strategy for making metal clusters encapsulated inside microporous solids selectively accessible to reactant molecules by manipulating the molecular sieve size and affinity for adsorbed molecule expands the catalytic capabilities of these materials to reactions demanding high selectivity and stability. Selective hydrogen combustion was achieved over Pt clusters encapsulated in LTA zeolite (KA, NaA, CaA) in a propene-rich mixture obtained from propane dehydrogenation and showed obvious pore-size dependent selectivity and coking rate. We found that propene tended to adsorb at channels or external surfaces of zeolite, interfering the diffusion of hydrogen and oxygen and thus lowering the catalyst activity. Tailoring the surface chemistry of LTA zeolite with additional alkali or alkaline earth oxides contributed to narrowing zeolite pore size and their affinity for propene. The modified Pt@KA catalyst with small pore size displayed excellent hydrogen combustion selectivity (98.5%) with high activity, superior anti-coking and anti-sintering properties.

Eliminating undesirable by-products to achieve high selectivity and energy efficiency is the main goal of heterogeneous catalysis but remains a challenge<sup>[1]</sup>. Decades of research have led to fundamental approaches to facilitate a preferred reaction pathway towards targeted products. Driven by the demand for highly selective and stable metal clusters, researchers have increasingly been drawn towards metal clusters encapsulated in zeolite (cluster@zeolite)<sup>[2]</sup>. Confining metal clusters within the cavities of zeolite can allow active sites to select reactants and transition states based on molecular size and protect such clusters against sintering<sup>[3]</sup>. However, as we and others found that the catalytic efficiency of these catalysts was significantly lowered in the presence of competitive reactants interacting strongly with zeolite<sup>[2c,4]</sup>, such as in the case of methanol oxidative dehydrogenation on Na(RuO<sub>2</sub>)A in presence of 2-methyl-1-propanol<sup>[2c]</sup>, 1-hexene hydrogenation on silicalite-1 coated Pt/TiO<sub>2</sub> catalyst in presence of 3,3-dimethylbut-1-ene<sup>[4a]</sup>, naphthalene hydrogenation on mesoporous KA encapsulated Pt catalyst in presence of dibenzothiophene<sup>[4b]</sup>. Hydrocarbons with larger size tend to interfere with other reactants diffusion into zeolite channels<sup>[2c, 4a,5]</sup>. Although often observed in literatures,

the lowered catalytic efficiency has not been addressed, it is highly desired to explore such catalysts to utilize the encapsulated catalysts more effectively.

As an on-purpose technology for propene production, propane dehydrogenation (PDH) has become an attractive option to fill the widening gap between the increasing demand for propene and the decreasing production from steam crackers and fluid catalytic cracking units<sup>[6]</sup>. PDH is endothermic and limited by chemical equilibrium. Selective hydrogen combustion (SHC)<sup>[7]</sup>, or oxidative dehydrogenation (ODH)<sup>[8]</sup>, has the advantages of oxidizing hydrogen in-situ to shift the chemical equilibrium and enhance the process energy efficiency<sup>[7,8]</sup>. Metal oxides<sup>[9]</sup> and precious metal catalysts<sup>[10]</sup>, such as Au<sup>[10a]</sup> and Pt<sup>[10b-e]</sup> have been intensively studied for SHC. Among them Pt-based catalysts have shown the best performances. For all the above mentioned catalysts, their abilities to selective oxidation of hydrogen from hydrocarbon mixtures depend on their intrinsic catalytic properties, which tend to be limited by the presence of propene<sup>[9,10]</sup>. In addition, maintaining the catalytic active phases of catalysts under hydrothermal conditions is another challenge<sup>[11]</sup>.

Herein, we report the design and modification principles of a kind of catalyst for SHC in hydrocarbon mixtures by embedding Pt clusters within zeolite and applying the molecular sieving effect, as shown in Figure 1a. It allows only H<sub>2</sub> and O<sub>2</sub> access to the Pt clusters while excludes hydrocarbons. Based on the reactant kinetic diameter (0.29 nm, 0.35 nm, 0.43 nm, 0.45 nm for H<sub>2</sub>, O<sub>2</sub>, C<sub>3</sub>H<sub>8</sub>, C<sub>3</sub>H<sub>6</sub>, respectively), Linde type A (LTA) zeolites with effective pore size similar or smaller than 0.43 nm (0.43 nm, 0.41 nm and 0.3 nm for CaA, NaA and KA, respectively) that are prospect of sieving H<sub>2</sub> and O<sub>2</sub> from hydrocarbons were selected as shell matrix. The experimental and DFT study revealed that the zeolite pore size and its affinity for propene are two crucial factors influencing the selectivity, activity and coking rate of Pt@LTA catalyst. After tuning the surface chemistry of shell zeolite with alkali oxides, the selectivity of Pt@KA with smallest pore size reaches an outstanding level of 98.5%, much higher than that on Pt/SiO<sub>2</sub> catalyst (83.7%) under the same propene-rich condition.

Encapsulation of Pt clusters within NaA was achieved via hydrothermal synthesis using ligand-stabilized platinum precursors<sup>[2a,2g]</sup>. Pt@KA and Pt@CaA catalysts were obtained through ion-exchange of Pt@NaA with corresponding salts<sup>[2a]</sup>. Pt supported on SiO<sub>2</sub> was prepared by incipient wetness impregnation. The physicochemical properties of all catalysts are provided in the Supporting Information (Table S1). The high-resolution transmission electron microscopy (TEM) showed that the mean Pt particle sizes were 1.1 nm, 1.4 nm and 1.1 nm for Pt@NaA, Pt@KA and Pt@CaA, respectively (Figure 1b, Figure S1). Pt clusters are narrowly distributed and most of them are similar to the dimension of  $\alpha$  cage in LTA zeolites. Besides, no obvious changes in Pt size were observed after surface modification with additional alkali or alkaline earth oxides. Energy dispersive X-ray spectroscopy (EDS) analysis showed an uniform distribution of Pt in zeolite (Figure S2). X-ray

[\*] Dr. Y. Shan  
State Key Laboratory of Chemical Engineering, East China University of Science and Technology, 130 Meilong Road, Shanghai, 200237 (China); College of Materials Science and Engineering, Qingdao University, 308 Ningxia Road, Qingdao 266073, China.  
Prof. Dr. Z. Sui, Prof. Dr. Y. Zhu, Prof. Dr. J. Zhou, Prof. X. Zhou  
State Key Laboratory of Chemical Engineering, East China University of Science and Technology, 130 Meilong Road, Shanghai, 200237 (China)  
E-mail: zhjsui@ecust.edu.cn

[\*\*] Prof. Dr. D. Chen  
Department of Chemical Engineering, Norwegian University of Science and Technology, Trondheim 7491 (Norway)  
E-mail: de.chen@ntnu.no

diffraction (XRD) (Figure 1c) revealed the high crystallinity of shell zeolites, but no peaks could be assigned to Pt phases, suggesting their high dispersion. In addition, PDH was used as a model reaction to assess the degree of Pt encapsulation. It was found that the TOFs of PDH on Pt@CaA, Pt@NaA and Pt@KA is 0.09, 0.02 and 0.007 times of that on Pt/SiO<sub>2</sub>, respectively (Figure 1d). These results together indicate the successful encapsulation of Pt clusters within zeolite. **Pt clusters larger than cage dimensions of A zeolite can also be found and these metal clusters most likely also embedded in the zeolite crystals, similar to ones observed previously [2].**

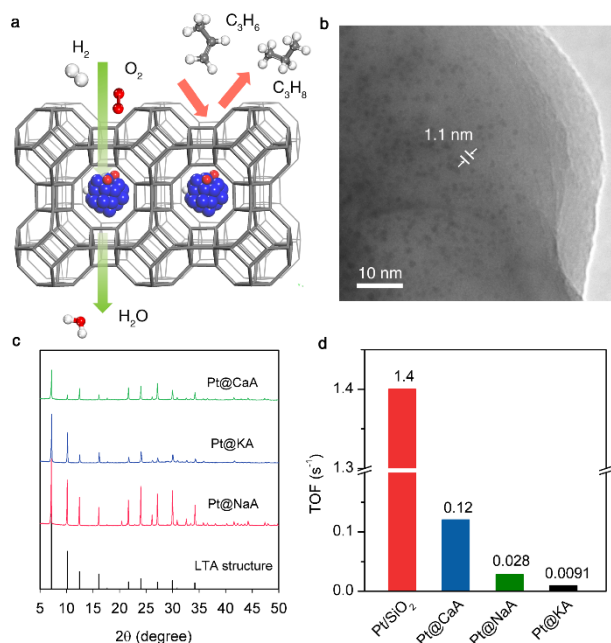


**Figure 1.** (a) Schematic illustration of the design concept for the SHC catalyst: Pt encapsulated in a dense support matrix that allows selective diffusion of H<sub>2</sub> and O<sub>2</sub> over hydrocarbons. (b) TEM image of the Pt@NaA. (c) XRD patterns of the Pt@LTA. (d) TOFs of PDH over Pt/SiO<sub>2</sub> and Pt@LTA catalysts.

The SHC was performed on Pt/SiO<sub>2</sub>, Pt@LTA (Pt@CaA, Pt@NaA and Pt@KA) and alkaline or alkaline earth oxides modified catalysts (Pt-3Ca@CaA, Pt-3Na@NaA and Pt-3K@KA) in a mixture of hydrogen, propane and propene, where the composition is equivalent to the propane conversion of 60% in PDH. The selectivity (O<sub>2</sub> selectivity over water) and activity (conversion of O<sub>2</sub>) of these catalysts at steady-state stage after 25 hours on stream, and coke amount accumulated on spent catalysts were summarized in Figure 2. It can be concluded that the performances of these catalysts varied strongly between different catalysts. The selectivity of Pt@LTA catalysts before and after modification increased concurrently with the reduced pore sizes of the LTA zeolites. The highest selectivity (98.5%) was achieved on Pt-3K@KA with the smallest pore size, which is much higher than that (83.7%) on Pt/SiO<sub>2</sub>. The activity of modified Pt@LTA catalysts was high (93.3%, 92.8% and 83.5% for Pt-3K@KA, Pt-3Na@NaA and Pt-3Ca@CaA, respectively) and comparable to that on Pt/SiO<sub>2</sub> (96.6%).

The unexpected performances of Pt@LTA catalysts were observed where the selectivity of Pt@NaA and Pt@CaA was even lower than that on Pt/SiO<sub>2</sub> (Figure 2). In addition, the activity of Pt@LTA was much lower than that on Pt/SiO<sub>2</sub>. However, when SHC occurs in a mixture of hydrogen and propane without propene, the performances of Pt@LTA became quite different and the shape selective oxidation was unambiguously observed (Figure S3). The selectivity of Pt/SiO<sub>2</sub> was the lowest among all tested catalysts, while that of Pt@LTA increased with decrease of the zeolite pore size. Almost 100% O<sub>2</sub> selectivity over water was achieved on Pt@KA. Therefore, propene molecules obviously inhibited the SHC reaction.

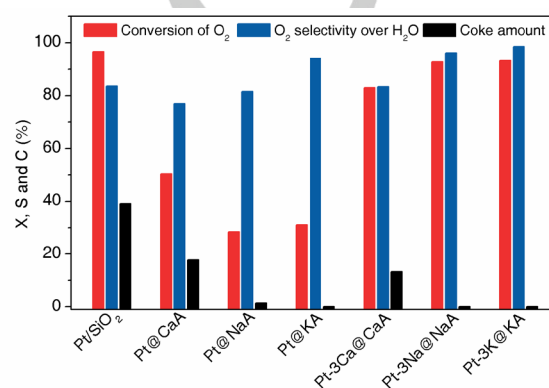


**Figure 2.** Conversion of O<sub>2</sub> (X, red) and O<sub>2</sub> selectivity over H<sub>2</sub>O (S, blue) at steady-state stage for SHC on Pt/SiO<sub>2</sub>, Pt@LTA and Pt-3M/LTA (M=Ca, Na or K) catalysts under propene-rich condition; coke amount (C, black) accumulated on spent catalysts after 25 hours on stream.

To understand the unexpected catalytic behaviour of Pt@LTA in the presence of propene, the evolution of activity and selectivity was investigated (Figure 3). It was found that the activity of Pt@LTA decreased rapidly, while the selectivity of them increased significantly with time on stream. Generally, the loss of catalytic activity correlates with sintering of Pt clusters<sup>[11,12]</sup> or coke accumulation on the surface of catalyst<sup>[8,12]</sup>. The HAADF-STEM image of spent Pt@NaA after 120 hours on stream showed that the diameter of the majority of Pt clusters remained to be 1.1 nm, while that of Pt particles supported on silica aggregated rapidly from 2.3 nm to 6.1 nm after only 25 hours on stream (Figure S4). This result clearly showed the superior sintering-resistance of encapsulated Pt clusters, consistent with literature observations<sup>[2d,2e,3]</sup>. The coke amount on spent catalysts determined by TG analysis for Pt/SiO<sub>2</sub>, Pt@CaA and Pt@NaA was 39.1 wt%, 17.8 wt% and 1.42 wt%, respectively, and that on spent Pt@KA was beyond detection limitation (Figure 2, Table S2). It is clear that the coke amount is intimately correlated with the pore size of LTA zeolite, indicating the effectiveness of shell zeolite in suppressing coke formation from propene deep dehydrogenation<sup>[13]</sup>. Although covered by heavy cokes, the activity of Pt/SiO<sub>2</sub> retained high while the selectivity of it decreased rapidly over time (Figure S5). The loss of selectivity might be caused by graphitizing cokes that are capable of promoting non-selective propene oxidation<sup>[14]</sup>. Even though the coke was not detected on Pt@KA, a rapid decrease

in activity was observed. Therefore, neither sintering of Pt clusters nor the coke accumulation is responsible for the observed low SHC activity of Pt@LTA catalysts in the presence of propene.

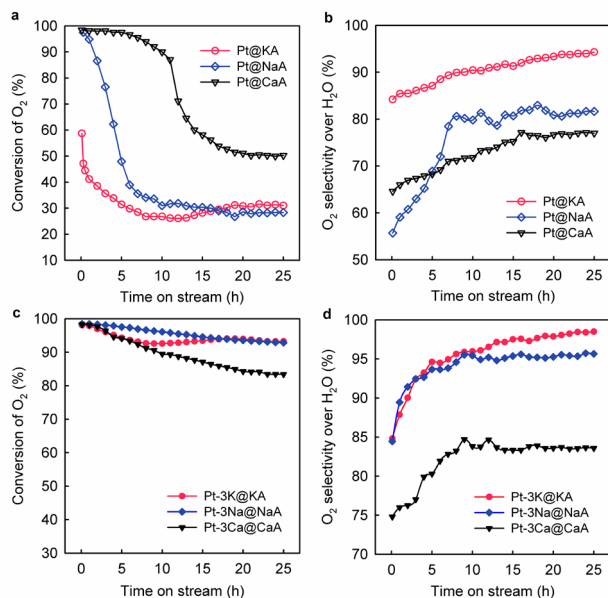


**Figure 3.** Hydrogen combustion over Pt@LTA and Pt-3M/LTA (M=Na, K or Ca) catalysts under propene-rich condition: (a,c) Conversion of O<sub>2</sub>; (b,d) O<sub>2</sub> selectivity over H<sub>2</sub>O.

Temperature-programmed oxidation (TPO) of propene was performed over KA, NaA, CaA and SiO<sub>2</sub> to investigate the interaction of propene with zeolite (Figure S6). The oxidation of propene was negligible on SiO<sub>2</sub> and KA but was remarkable on NaA and CaA, which strongly suggested that propene could be oxidized on neat zeolites, probably at charge-balancing cations. Temperature-programmed desorption of ammonia (NH<sub>3</sub>-TPD) on fresh and spent Pt@NaA showed that both the acid strength and acid concentration decreased during the reaction (Figure S7). Therefore, the oxidation of propene on zeolite acid sites could contribute to the initial high level of oxygen conversion but low selectivity on Pt@LTA. The selectivity increased over time, as these acid sites were gradually deactivated by coking reactions such as oligomerization<sup>[15]</sup>.

The inhibition effect of propene was revealed by the kinetic study showed in Figure 4a. For all the Pt@LTA catalysts, the oxygen conversion decreased sharply as the propene partial pressure increased, and the inhibition effect was stronger for catalysts with smaller zeolite pore size. It is interesting to find that high oxygen conversion can be instantly restored when the propene partial pressure was decreased (Figure S8), clearly indicating the reversibility of deactivation by propene adsorption. The adsorption property of propene on LTA zeolites was revealed by the breakthrough curve analysis shown in Figure 4b. Pt@CaA showed the latest breakthrough and thus the highest capacity for propene. Pt/NaA showed early breakthrough but extremely slow propene adsorption rate. Propene adsorption on

Pt@KA was lowest among three Pt@LTA as indicated by early breakthrough point and steep breakthrough curve (Figure 4b, Figure S9). These results suggested that the adsorption of propene at channels or on the external surfaces of zeolite would block the access of hydrogen and oxygen to the encapsulated Pt clusters, resulting in low activity of Pt@LTA at steady-state stage.

Insights into the propene adsorption on LTA zeolite were provided by the density functional theory (DFT) calculation (Figure S10). The most favourable adsorption sites for propene with an adsorption heat of -40.0 kJ/mol are cations located on the top of 4-rings (S3), but which occupied only 1/12 of total acid sites<sup>[16]</sup>. Cations located inside 8-rings (S2) – the main channels of LTA zeolite has an adsorption heat of -30.6 kJ/mol. It was found that the most favorable propene adsorption configuration on this site was that it binds to the cation via its double bond and is further stabilized by a H-bond (R<sub>H-O</sub>=2.94 Å) between H atom on methyl group and a framework oxygen atom. Similar adsorption configuration was found on cations located inside 6-ring (S1). Since the adsorption of propene is stronger than that of hydrogen<sup>[17]</sup> and oxygen<sup>[18]</sup> on LTA zeolite, these adsorption configurations of propene would contribute to inhibiting the access of reagents and further to lowering the activity of Pt@LTA catalysts.

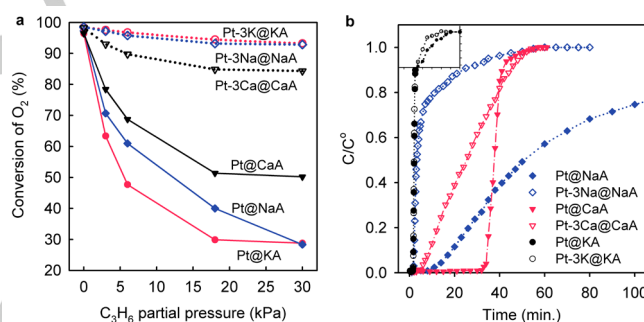


**Figure 4.** (a) Conversion of O<sub>2</sub> as a function of propene partial pressure for Pt@LTA and Pt-3M/LTA (M=Na, K) catalysts under propene-rich condition; (b) Propene breakthrough curves for Pt@LTA and Pt-3M/LTA (M=Na, K or Ca) catalysts with amplified curves of Pt@KA and Pt-3K@KA inserted within it.

To make the SHC more effective, it is essential to remove the blocking effect resulted from propene adsorption. The Pt@LTA catalysts were then modified by introducing additional alkali or alkaline earth oxides onto the external surface of zeolites. The same metal ions as those serving as charge balancing cations were used for the surface tuning to avoid pore size change of primary zeolite due to ion-exchange between them. Compared with Pt@LTA, Pt-3Na@NaA and Pt-3Ca@CaA had earlier breakthrough points and thus reduced propene adsorption amounts (Figure 4b). In addition, the slope of the breakthrough curve for Pt-3Ca@CaA tended to be flatter and that of Pt-3Na@NaA became much steeper, indicating the decrease of adsorption capacity and pore size was also achieved on Pt-3K@KA as indicated by slightly steeper breakthrough curve of it than Pt@KA (Figure 4b, Figure S9). Furthermore, the kinetic

dependence of SHC reaction was much less negative on propene partial pressure for all modified catalysts (Figure 4c). Therefore, this surface tuning strategy contributed to weakening of propene adsorption and narrowing of zeolite pore size. Accordingly, both the activity and the selectivity were remarkably improved on modified catalysts as shown in Figure 3c and 3d. The best performance was obtained on Pt-3K@KA catalyst with smallest zeolite pore size – none detectable coke amount, nearly full conversion of oxygen and almost complete selective combustion of hydrogen. The good durability of Pt-3K@KA was demonstrated over 100 hours on stream (Figure S11). Characterization of spent catalysts by XRD and HAADF-STEM showed that the structure of modified Pt@KA was stabilized after the initiation period and able to retain its structure characters in the long-run test (Figure S12).

In summary, we have demonstrated that highly selective hydrogen combustion in a propene-rich mixture can be achieved on Pt clusters encapsulated in modified LTA zeolite. The encapsulated Pt clusters showed obvious pore-size dependent selectivity and coking rate. Furthermore, the blocking effect of propene adsorbed at channels or on the external surfaces of zeolite was identified as main challenge for efficient SHC on encapsulated catalysts. Tuning the surface chemistry of zeolite with additional alkali or alkaline earth oxides was testified an effective way to weaken propene adsorption and narrow zeolite pore size. Significantly, together with the size exclusion and confining effect, the outstanding SHC activity, selectivity and durability on Pt-3K@KA were achieved. The strategy for engineering metal cluster confinement in zeolites developed here opens a new avenue to improve the catalytic efficiency of shape selective catalysts to make them practically applicable in industrially important reactions such as selective oxidation, hydrogenation and dehydrogenation in presence of competitive reactants or poisons for catalytic sites. Moreover, our findings are expected to radically improve current alkane dehydrogenation technologies by significantly increasing the per-pass yield of alkene in addition to in-situ supplying heat through selective hydrogen combustion.

## Acknowledgements

This work was financially supported by the National Natural Science Foundation of China (No. 91645122) and by the Natural Science Foundation of Shandong Province, China (No. ZR2017BB014). The supports from Norwegian research council and Norwegian University of Science and Technology are highly acknowledged.

**Keywords:** heterogeneous catalysis • encapsulation • selective hydrogen combustion • propane dehydrogenation • zeolites

- [1] G. A. Somorjai, J. Y. Park, *Angew. Chem. Int. Edit.* **2008**, *47*, 9212-9228; *Angew. Chem.* **2008**, *120*, 9352-9368.
- [2] a) P. B. Weisz, V. J. Frilette, R. W. Maatman, E. B. Mower, *J. Catal.* **1962**, *1*, 307-312; b) P. Collier, S. Golunski, C. Malde, J. Breen, R. Burch, *J. Am. Chem. Soc.* **2003**, *125*, 12414-12415; c) B. Z. Zhan, E. Iglesia, *Angew. Chem. Int. Edit.* **2007**, *46*, 3697-3700; *Angew. Chem.* **2007**, *119*, 3771-3774. d) M. Choi, Z. Wu, E. Iglesia, *J. Am. Chem. Soc.* **2010**, *132*, 9129-9137; e) J. Im, H. Shin, H. Jang, H. Kim, M. Choi, *Nat. Commun.* **2014**, *5*, 3370-3378; f) Z. Wu, S. Goel, M. Choi, E. Iglesia, *J. Catal.* **2014**, *311*, 458-468; g) L. Liu, U. Diaz, R. Arenal, G. Agostini, P. Concepcion, A. Corma, *Nat. Mater.* **2017**, *16*, 132-138; h) J. Zhang, L. Wang, Y. Shao, Y. Wang, B. C. Gates, F. S. Xiao, *Angew. Chem. Int. Edit.* **2017**, *56*, 9747-9751; *Angew. Chem.* **2017**, *129*, 9879-9883.
- [3] a) N. Kosinov, C. Liu, E. J. M. Hensen, E. A. Pidko, *Chem. Mater.* **2018**, *30*, 3177-3198; b) R. Qin, P. Liu, G. Fu, N. Zheng, *Small-Methods* **2018**, *2*, 1700286-1700306; c) T. Iida, D. Zanchet, K. Ohara, T. Wakihara, Y. Román-Leshkov, *Angew. Chem. Int. Edit.* **2018**, *57*, 6454-6458; *Angew. Chem.* **2018**, *130*, 6564-6568.
- [4] a) N. Nishiyama, K. Ichioka, D. H. Park, Y. Egashira, K. Ueyama, L. Gora, W. Zhu, F. Kapteijn, J. A. Moulijn, *Ind. Eng. Chem. Res.* **2004**, *43*, 1211-1215; b) T. He, Y. Wang, P. Miao, J. Li, J. Wu, Y. Fang, *Fuel*, **2013**, *106*, 365-371.
- [5] W. J. W. Bakker, F. Kapteijn, J. Poppe, J. A. Moulijn, *J. Membrane. Sci.* **1996**, *117*, 57-78.
- [6] J. J. H. B. Sattler, J. Ruiz-Martinez, E. Santillan-Jimenez, B. M. Weckhuysen, *Chem. Revs.* **2014**, *114*, 10613-10653.
- [7] R. K. Grasselli, D. L. Stern, J. G. Tsikoyiannis, *Appl. Catal. A-Gen.* **1999**, *189*, 1-8.
- [8] a) K. Chen, E. Iglesia, A. T. Bell, *J. Catal.* **2000**, *192*, 197-203; b) J. T. Grant, C. A., Carrero, F. Goettl, J. Venegas, P. Mueller, S. P. Burt, S. E. Specht, W. P. Mcdermott, A. Chiericato, I. Hermans, *Science* **2016**, *354*, 1570-1573.
- [9] a) J. G. Tsikoyiannis, D. L. Stern, R. K. Grasselli, *J. Catal.* **1999**, *184*, 77-86; b) J. H. Blank, J. Beckers, P. F. Collignon, F. Clerc, G. Rothenberg, *Chemistry* **2007**, *13*, 5121-5128; c) J. Beckers, R. Drost, I. V. Zandvoort, P. F. Collignon, G. Rothenberg, *Chemphyschem* **2008**, *9*, 1062; d) R. B. Dudek, Y. Gao, J. Zhang, F. Li, *AIChE. J.* DOI 10.1002/aic.16173.
- [10] a) H. Dyrbeck, N. Hammer, M. Rønning, E. A. Blekkan, *Top. Catal.* **2007**, *45*, 21-24; b) T. Waku, J. A. Biscardi, E. Iglesia, *J. Catal.* **2004**, *222*, 481-492; c) L. Lâte, J. I. Rundereim, E. A. Blekkan, *Appl. Catal. A-Gen.* **2004**, *262*, 53-61; d) S. Kaneko, T. Arakawa, M. A. Ohshima, H. Kurokawa, H. Miura, *Appl. Catal. A-Gen.* **2009**, *356*, 80-87; e) M. L. Yang, C. Fan, Y. A., Zhu, Z. J. Sui, X. G. Zhou, D. Chen, *J. Phys. Chem. C* **2015**, *119*, 21386-21394.
- [11] a) J. Barbier, D. Duprez, *Appl. Catal. B-Environ.* **1994**, *4*, 105-140; b) Y. Shan, Z. Sui, Y. Zhu, D. Chen, X. Zhou, *Chem. Eng. J.* **2015**, *278*, 240-248; c) Y. L. Shan, Y. A. Zhu, Z. J. Sui, D. Chen, X. G. Zhou, *Catal. Sci. & Technol.* **2015**, *5*, 3991-4000.
- [12] H. Xiong, S. Lin, J. Goetze, P. Pletcher, H. Guo, L. Kovarik, K. Artyushkova, B. M. Weckhuysen, A. K. Datye, *Angew. Chem. Int. Edit.* **2017**, *56*, 8986-8991; *Angew. Chem.* **2017**, *129*, 9114-9119.
- [13] L. Nykänen, K. Honkala, *ACS Catal.* **2013**, *3*, 3026-3030.
- [14] F. J. Maldonado-Hódar, L. M. P. Madeira, M. F. Portela, *J. Catal.* **1996**, *164*, 399-410.
- [15] a) Y. G. Kolyagin, V. V. Ordonsky, Y. Z. Khimyak, A. I. Rebrov, F. Fajula, I. I. Ivanova, *J. Catal.* **2006**, *238*, 122-133; b) G. L. Price, V. Kanazirev, K. M. Dooley, V. I. Hart, *J. Catal.* **1998**, *173*, 17-27.
- [16] R. Y. Yanagida, A. A. Amaro, K. Seff, *J. Phys. Chem.* **1973**, *77*, 805-809.
- [17] C. O. Areán, G. T. Palomino, M. R. L. Carayol, A. Pulido, M. Rubeš, O. Bludský, P. Nachtigall, *Chem. Phys. Lett.* **2009**, *477*, 139-143.
- [18] S. P. Nandi, P. L. Walker Jr., *Sep. Sci. Technol.* **1976**, *11*, 441-453.

## Table of Contents

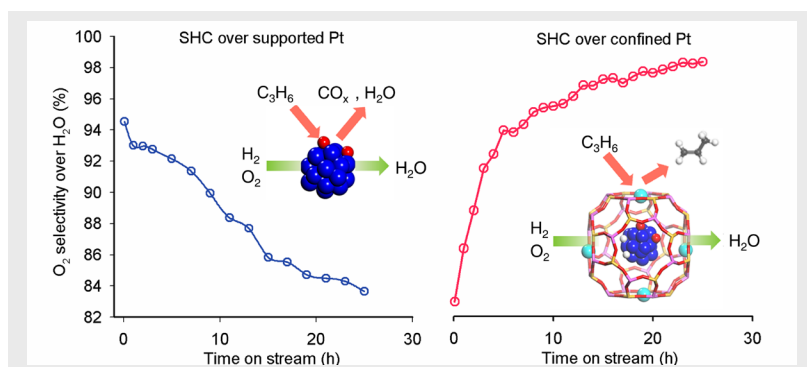
Layout 2:

## COMMUNICATION

Yuling Shan, Zhijun Sui\*, Yian Zhu,  
Jinghong Zhou, Xingui Zhou and De  
Chen\*

Page No. – Page No.

**Boosting size-selective hydrogen  
combustion in presence of propene  
using controllable metal clusters  
encapsulated in zeolite**



This paper describes the design and modification of zeolite-encapsulated Pt clusters as selective hydrogen combustion catalyst. Pt clusters confined in LTA zeolite showed pore-size dependent selectivity and coking rate, but their activity was suppressed by propene adsorption revealed by kinetic and DFT study. After removing the blocking effect of propene by surface modification, encapsulated Pt clusters can serve as efficient SHC catalysts with high selectivity, superior anti-coking and anti-sintering properties.